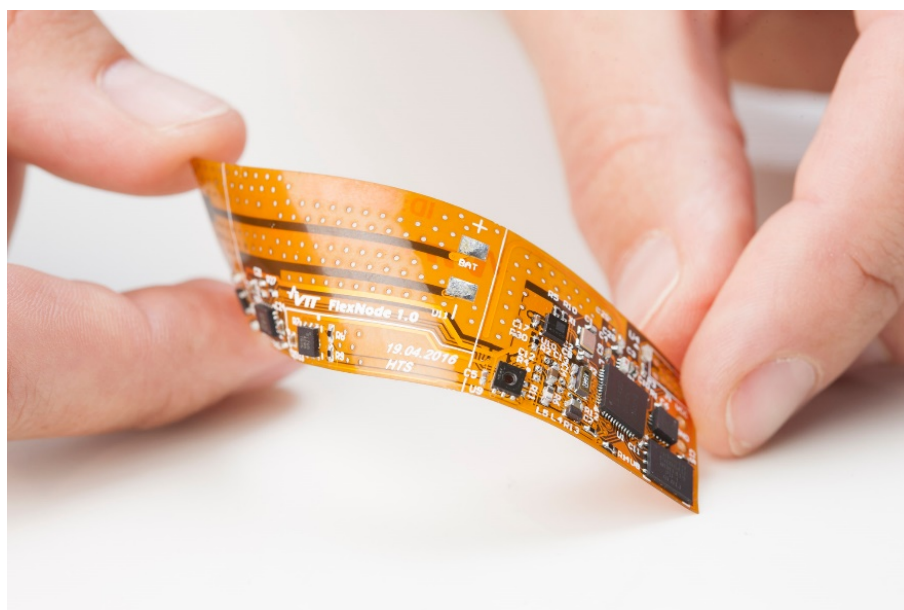


## RESEARCH REPORT

VTT-R-01051-21



# Reaction kinetics of antioxidants for polyolefins

Authors: Jukka Vaari

Confidentiality: VTT Public

Version: 24.11.2021

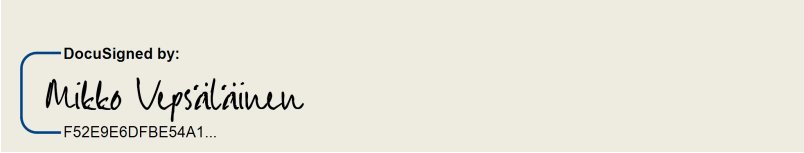


<b>Report's title</b> Reaction kinetics of antioxidants for polyolefins	
<b>Customer, contact person, address</b> SAFIR2022	<b>Order reference</b>
<b>Project name</b> SAMPO	<b>Project number/Short name</b> 129019/SAFIR2022_SAMPO 2021
<b>Author(s)</b> Jukka Vaari	<b>Pages</b> 24
<b>Keywords</b> Antioxidants, polyolefins, oxidative degradation	<b>Report identification code</b> VTT-R-01051-21
<p><b>Summary</b></p> <p>This report presents a literature survey on antioxidants intended to provide protection against oxidative degradation of polyolefin materials, and in particular, the reaction kinetics involved. Since antioxidants are designed to react with the intermediate products of the polyolefin degradation reaction rather than oxygen, an introduction to the oxidative degradation kinetics of unstabilized polyolefin materials is first given. A kinetic model describing oxidative degradation of pure polymer material is presented, and an example simulation on thermal ageing is conducted.</p> <p>This is followed by an introduction of the main types of antioxidants, with the main focus on their chemical structure and reactivity, but information on their physical properties is also provided. Subsequently, equations describing the inhibiting action of antioxidants are introduced into the kinetic model. The model is used to simulate the oxidative induction time experiment of both fresh and aged materials, as well as thermal and thermo-radiative ageing of materials.</p> <p>The main assumptions of the kinetic model presented in this report are oxygen excess and homogeneous distribution of reacting species. Effects arising from transport limitations are excluded, but need to be included in further work. A particular issue requiring further work is related to possible chemical ineffectiveness and/or transport limitations of antioxidants, which could lead to oxidative degradation despite significant levels of antioxidant remaining in the material.</p>	
<b>Confidentiality</b>	VTT Public
Espoo 25.1.2022	
<b>Written by</b>  Jukka Vaari Senior Scientist	<b>Reviewed by</b>  Konsta Sipilä Senior Scientist
<b>VTT's contact address</b> Jukka Vaari, Vuorimiehentie 2, PO Box 1000, FI-02044 VTT, jukka.vaari@vtt.fi, +358405233692	
<b>Distribution (customer and VTT)</b> SAFIR2022, 1 VTT achive, 1	
<p><i>The use of the name of "VTT" in advertising or publishing of a part of this report is only permissible with written authorisation from VTT Technical Research Centre of Finland Ltd.</i></p>	



## Approval

### VTT TECHNICAL RESEARCH CENTRE OF FINLAND LTD

Date:	25 January 2022
Signature:	 A DocuSign signature block for Mikko Vepsäläinen. It features a blue bracket on the left containing the text 'DocuSigned by:' above the handwritten signature 'Mikko Vepsäläinen' in black ink. Below the signature is the alphanumeric string 'F52E9E6DFBE54A1...'. The entire block is set against a light beige background.
Name:	Mikko Vepsäläinen
Title:	Research Team Leader



## Contents

---

1. Introduction.....	4
2. Oxidative degradation of polyolefins .....	4
2.1 Standard oxidative degradation mechanism .....	4
2.2 Initiation.....	5
2.3 Propagation.....	6
2.4 Termination .....	6
2.5 Kinetic model.....	6
3. Antioxidants.....	9
3.1 Primary antioxidants .....	9
3.1.1 Phenolic antioxidants .....	10
3.1.2 Secondary aromatic amines.....	13
3.1.3 Hindered amine light stabilizers.....	14
3.2 Secondary antioxidants .....	14
3.3 Multi-functional antioxidants.....	15
3.4 Physical properties of antioxidants.....	15
4. Reaction kinetics of antioxidants.....	17
4.1 Reaction mechanisms .....	17
4.2 Kinetic modelling of phenolic antioxidants.....	18
5. Summary .....	21
References.....	22

## 1. Introduction

---

This report presents a literature survey on antioxidants intended to provide protection against oxidative degradation of polyolefin materials, and in particular, the reaction kinetics involved. Oxidative degradation of polyolefin materials may occur during the entire lifespan of the materials, including synthesis and processing stages, as these typically involve high temperatures under ambient air. When materials become final products, these may be stored for long times before being sold to end use. While the stability of materials during the expected service life is the goal, the role of antioxidants and other stabilizers during earlier stages is important and affects the required amount of additives initially mixed in the material.

In order to understand how antioxidants work, it is necessary to review the oxidative degradation mechanism of polyolefins. Antioxidants are not designed to react with oxygen (although they may do so), but rather with the intermediate products of the polyolefin degradation reaction, and therefore reaction kinetics of antioxidants cannot be separated from the oxidative degradation kinetics of polyolefins.

This report, therefore, starts with an introduction to the oxidative degradation kinetics of unstabilized polyolefin materials. This is followed by an introduction of the main types of antioxidants, with a particular focus on their chemical structure and reactivity. Subsequently, oxidative degradation mechanisms are presented that include the effect of antioxidants. Furthermore, these models are used to calculate examples of antioxidant depletion as a function of initial antioxidant concentration and temperature under oxygen excess conditions, i.e. conditions where oxygen concentration in the material is limited only by solubility, and not by diffusion.

## 2. Oxidative degradation of polyolefins

---

### 2.1 Standard oxidative degradation mechanism

The degradation under an oxidative environment of organic polymers has been studied extensively. How the details of the mechanism are presented depends somewhat on the author. The presentation in this report builds on the comprehensive treatise on the subject due to Verdu (2013), and a more concise presentation limited to thermal oxidation given by Colin and Verdu (2012). The oxidation of organic polymers results from a radical chain mechanism involving three steps:

- Initiation: non-radical species  $\rightarrow$  radicals
- Propagation: one radical  $\rightarrow$  one radical
- Termination: two radicals  $\rightarrow$  non-radical species

The 'standard' reaction mechanism involves the following reactions.

Initiation:

- $RH \rightarrow R\cdot + H\cdot$  (1a)
- $\delta ROOH \rightarrow \alpha R\cdot + \beta ROO\cdot$  (1b)

Propagation:

- $R\cdot + O_2 \rightarrow ROO\cdot$  (2)
- $ROO\cdot + RH \rightarrow ROOH + R\cdot$  (3)

Termination:

- $R_1\cdot + R_2\cdot \rightarrow R_1-R_2 + X$  (4)
- $R_1\cdot + R_2OO\cdot \rightarrow R_1-O-O-R_2 + X$  (5)
- $R_1OO\cdot + R_2OO\cdot \rightarrow R_1-O-O-R_2 + O_2 + X$  (6)



where R stands for a radical, and the dot explicitly denotes an unpaired valence electron.  $\delta$ ,  $\alpha$ , and  $\beta$  in equation (1b) are integers. The X in equations (4-6) explicitly denotes a cross-link event.

## 2.2 Initiation

The two initiation reactions (1a) and (1b) describe radiative and oxidative reactions, respectively. It is stressed by Verdu (2013) that these should be regarded as initial reaction steps of a reaction scheme, and not necessarily the fundamental phenomena that lead to initiation. In the case of the radiative pathway (1a), a C-H bond scission is due either to primary electromagnetic radiation or to primary or secondary electrons. It is conceptually simple, because it involves just a dose rate, with no assumptions on the initial state of the polymer. The coupling between dose rate and reaction rate is established by measuring the radiochemical yield of hydrogen gas,  $G(\text{H}_2)$  during irradiation. The units of G are the number of molecules per 100 eV of energy absorbed. Taking into account that the formation of a hydrogen molecule requires the formation of two radicals, one arrives at a rate expression for initiation:  $r_i \approx 10^{-7}GD$  where D is the dose rate (Gy/s), and  $r_i$  has the units mol/l/s (Khelidj et al. 2006).

The oxidative pathway is philosophically more challenging, for equation (1b) assumes that hydroperoxide species exist at  $t=0$ . Furthermore, hydroperoxides are produced by the propagation reaction (3). It is suggested by Colin and Verdu (2012) that the fundamental phenomena leading to the presence of these hydroperoxides are impossible to establish because concentrations are too low to be measurable. According to Khelidj et al. (2005), polymers, especially industrially processed materials, always contain trace amounts of hydroperoxides or other unstable species, for otherwise their tendency to oxidize (either thermally or radiatively) could not be explained. Celina et al. (2013) have criticized the assumption of initial hydroperoxides especially in the case of high-temperature degradation, as hydroperoxides should decompose. Celina et al. have further expressed doubts on the high values of initial hydroperoxide concentrations required for kinetic models. Ahmad et al. (2014) note that high-temperature processing stages of polyolefins will lead to radical formation according to equation (1a) but with temperature and mechanical stress as the driving force. They accordingly assume an initial small concentration of R· radicals in their kinetic model, but acknowledge that these quickly react according to reactions (2) and (3) to form hydroperoxides.

It is customary in the reaction schemes by Verdu's group to somewhat simplify the reactions shown. This involves lumping together elementary reactions and leaving out some inactive and volatile reaction products. Thus, in a more explicit presentation, the unimolecular hydroperoxide decomposition reaction (1b) reads

- $\text{ROOH} \rightarrow \text{RO}\cdot + \text{OH}\cdot$
- $\text{HO}\cdot + \text{RH} \rightarrow \text{R}\cdot + \text{H}_2\text{O}$
- $\text{RO}\cdot + \text{RH} \rightarrow \text{ROH} + \text{R}\cdot$
- $\text{RO}\cdot \rightarrow \text{R}_1=\text{O} + \text{R}_2 + \text{S}$
- Balance:  $\text{ROOH} \rightarrow 2\text{R}\cdot + \text{H}_2\text{O} + (1 - \gamma_{\text{CO}}) \text{ROH} + \gamma_{\text{CO}}\text{RO} + \gamma_{\text{s}}\text{S}$

where S denotes chain scission event, and  $\gamma_{\text{CO}}$  and  $\gamma_{\text{s}}$  are the selectivities of the  $\text{RO}\cdot$  radical decomposition into a carbonyl and chain scission. The above equations suggest  $\gamma_{\text{CO}} = \gamma_{\text{s}}$ , but in practical modelling, differing values are used (Mikdam et al. 2017, Hettal et al. 2021). Similarly, the bimolecular reaction can be expanded as

- $\text{ROOH} + \text{ROOH} \rightarrow \text{RO}\cdot + \text{ROO}\cdot + \text{H}_2\text{O}$
- $\text{RO}\cdot + \text{RH} \rightarrow \text{ROH} + \text{R}\cdot$
- $\text{RO}\cdot \rightarrow \text{R}_1=\text{O} + \text{R}_2 + \text{S}$
- Balance:  $\text{ROOH} + \text{ROOH} \rightarrow \text{R}\cdot + \text{H}_2\text{O} + \text{ROO}\cdot + (1 - \gamma_{\text{CO}}) \text{ROH} + \gamma_{\text{CO}}\text{RO} + \gamma_{\text{s}}\text{S}$

Therefore, the initiation reaction (1b) ignores the formation of the inactive species (water, alcohols, carbonyls,...) no longer participating in the free radical process. It is seen that the integers of equation (1b) are ( $\delta=1$ ,  $\alpha=2$ ,  $\beta=0$ ) for unimolecular and ( $\delta=2$ ,  $\alpha=1$ ,  $\beta=1$ ) for bimolecular pathways. A few points are

**beyond the obvious**

worth mentioning. In the first step, hydroperoxide decomposes by homolytic dissociation of the O-O bond, creating two radicals. Therefore, hydroperoxide dissociation is not a chain scission or a disproportionation reaction, as suggested by (1b). Unimolecular decomposition dominates at high temperatures (low ROOH thermal stability) whereas bimolecular decomposition dominates at low temperatures.

The fourth (third) step on the unimolecular (bimolecular) scheme involves a chain  $\beta$ -scission (Walling & Padwa 1963), which competes with alcohol formation. Chain scission leads to the formation of carbonyl, giving a convenient way of experimentally (FTIR) following the progress of scission reactions by monitoring the carbonyl group vibration.

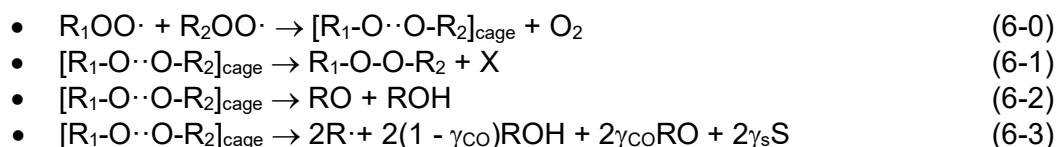
## 2.3 Propagation

The propagation reactions are due to the extraordinary properties of the oxygen molecule (Borden et al. 2017). Reaction (2) occurs between a polymer radical and molecular oxygen to form a peroxy radical. Notably, it involves neither dissociation of the oxygen molecule, nor hydrogen abstraction from the polymer. The oxygen molecule is a diradical, a species with two unpaired electrons in the valence orbital. While thermodynamically stable by itself, it reacts exothermically with almost any element. However, the activation energy is high, as exemplified by the fact that mixtures of oxygen and organic molecules require high (autoignition) temperatures before the reaction begins. Once peroxy radicals are formed, they readily react with other molecules through reaction (3).

Reaction (3) produces a hydroperoxide. Given that hydroperoxide is a species involved in the initiation reaction (1b), the degradation reaction scheme is autocatalytic by nature. This also means that from the kinetics modelling point of view, the first trace amounts of hydroperoxide are important only in the sense that they exist. Once the degradation process starts, the amount of hydroperoxide starts to increase, and the chain reaction accelerates until a steady-state value for the hydroperoxide concentration is reached. Hydroperoxide decomposition therefore also dictates the length of the induction period.

## 2.4 Termination

Termination reactions are couplings of two radical species to form inactive species no longer participating in the free radical process. Reaction (4) leads to a direct cross-link between chains, whereas reactions (5) and (6) lead to a cross-link with an -O-O- bridge. Kinetically, the reactivity of the radical  $R\cdot$  is greater than the reactivity of  $ROO\cdot$  so the rate of the termination reactions is (4) > (5) > (6). Reaction (6) is postulated to involve an intermediary  $R_1-O-O-O-R_2$  structure which is thermally unstable and quickly decomposes into a  $[R_1-O\cdot\cdot O-R_2]_{\text{cage}}$  structure and an  $O_2$  molecule. One of the particular properties of the  $O_2$  diradical molecule noted by Borden et al. (2017) is that despite  $O_2$  being a diradical, it does not form stable oligomers (as opposed, for example, to sulphur  $S_8$ ). The subscript 'cage' refers to the Franck-Rabinovich cage effect (Braden et al. 2001) where radicals are confined close to each other by surrounding molecules. Again, a more explicit representation of reaction (6) can be written as



which in addition to hydroperoxide formation shows two reaction paths leading to an alcohol and a carboxyl, one of which involves radical formation through chain scissions.

## 2.5 Kinetic model

Based on the mechanistic scheme presented above, a system of differential equations can be written that describes the time evolution of the species concentrations (Mikdam et al. 2017):

$$\frac{d[R \cdot]}{dt} = G \cdot 10^{-7} \cdot I + 2k_{1u}[ROOH] + k_{1b}[ROOH]^2 - k_2[O_2][R \cdot] + k_3[ROO \cdot][RH] - 2k_4[R \cdot]^2 - k_5[R \cdot][ROO \cdot] + 2k_{63}[ROOR]_{cage}$$

$$\frac{d[ROO \cdot]}{dt} = k_{1b}[ROOH]^2 + k_2[O_2][R \cdot] - k_3[ROO \cdot][RH] - 2k_4[R \cdot]^2 - k_5[R \cdot][ROO \cdot] + 2k_{60}[ROO \cdot]^2$$

$$\frac{d[ROOH]}{dt} = -k_{1u}[ROOH] - 2k_{1b}[ROOH]^2 + k_3[ROO \cdot][RH] - 2k_4[R \cdot]^2 - k_5[R \cdot][ROO \cdot]$$

$$\frac{d[ROOR]_{cage}}{dt} = k_{60}[ROO \cdot]^2 - (k_{61} + k_{62} + k_{63})[ROOR]_{cage}$$

$$\frac{d[O_2]}{dt} = -k_2[O_2][R \cdot] + 2k_{60}[ROO \cdot]^2$$

Here, the factors  $k$  are the rate constants of reactions (1-6) written above in 2.4, with  $k_{1u}$  and  $k_{1b}$  associated with uni- and bimolecular hydroperoxide decomposition reactions, respectively. The carbonyl concentration, and the concentration of cross-linking and chain scission events can be computed using the solution of the above equations:

$$\frac{d[C = O]}{dt} = \gamma_{CO}(k_{1u}[ROOH] + k_{1b}[ROOH]^2) + \gamma_{CO}2k_{63}[ROOR]_{cage}$$

$$\frac{dS}{dt} = \gamma_S(k_{1u}[ROOH] + k_{1b}[ROOH]^2) + \gamma_S2k_{63}[ROOR]_{cage}$$

$$\frac{dX}{dt} = \gamma_X k_4[R \cdot]^2 + \gamma_X k_5[R \cdot][ROO \cdot] + k_{61}[ROOR]_{cage}$$

In the above set of equations,  $[RH]$  stands for the concentration of methylene groups, and  $[O_2]$  for oxygen concentration. The set of equations assumes a low degree of oxidation, with  $[RH]$  remaining essentially constant, and oxygen excess, meaning that oxygen transport does not limit the rate of degradation reactions, meaning that  $[O_2]$  is also constant. Assuming a density of  $0.84 \text{ g/cm}^3$  for amorphous polyethylene, the concentration of methyl groups becomes  $[RH]=60 \text{ mol/l}$ . The oxygen concentration can be obtained as the product of oxygen partial pressure in air ( $0.21 \cdot 10^5 \text{ Pa}$ ) with oxygen solubility in amorphous PE ( $1.8 \cdot 10^{-8} \text{ mol/l/Pa}$ ), giving  $[O_2]=3.8 \cdot 10^4 \text{ mol/l}$  (Hettal et al. 2021). A high degree of oxidation would require adding an equation for  $[RH]$  depletion, and diffusion-limited oxidation would require adding a diffusive term to the equation for  $[O_2]$  (Mikdam et al. 2017), both of which are beyond the scope of this report.

Parameters for the kinetic model are listed in Table 1. While the rate constants appear consistent from one publication to another, the values for the yields  $\gamma$  seem to vary a great deal (Kheldij et al. 2006, Hettal et al. 2021), and without a clear trend as a function of temperature, so the values reported in Table 1 should be regarded with some caution.



Table 1. Parameters of the kinetic model.

	Pre-exponential factor (1/s or l/mol/s)	Activation energy (kJ/mol)	Reference
k1u	$8.0 \cdot 10^{12}$	140	Khelidj et al. 2006
k1b	$2.8 \cdot 10^9$	105	Khelidj et al. 2006
k2	$1.0 \cdot 10^8$	0	Khelidj et al. 2006
k3	$1.5 \cdot 10^{10}$	73	Khelidj et al. 2006
k4	$8.0 \cdot 10^{11}$	0	Richaud 2013
k5	$2.3 \cdot 10^{11}$ $1.8 \cdot 10^{11}$	0 0	Richaud 2013 Mikdam et al. 2017
k60	$4.9 \cdot 10^{19}$	80	Khelidj et al. 2006
k61	$2.0 \cdot 10^6$	0	Khelidj et al. 2006
k62	$1.2 \cdot 10^6$	5	Khelidj et al. 2006
k63	$8.0 \cdot 10^{12}$ $4.8 \cdot 10^9$	50 17.4	Khelidj et al. 2006 Colin et al. 2009
	Value		
$\gamma_{CO}$ (@ 60 °C)	1.0		Mikdam et al. 2017
$\gamma_S$ (@ 60 °C)	0.41		Mikdam et al. 2017
$\gamma_4$ (@ 60 °C)	0.50		Mikdam et al. 2017
$\gamma_5$ (@ 60 °C)	0.011		Mikdam et al. 2017

To illustrate how the model works, let us consider the thermal ageing in normal air of linear polyethylene with a mass-average molecular weight of  $M_w=100$  kg/mol, under a temperature of  $T=100$  °C. Since no radiation is involved, only the hydroperoxide decomposition reactions are involved in the initiation stage. This requires choosing a small but non-zero initial concentration of hydroperoxides, which is taken as  $[ROOH]_0=10^{-4}$  mol/l. The ode23s stiff solver of Matlab was used.

Results of the simulation are shown in Figure 1 for up to 30 days of ageing time. Although the model can calculate further, the results beyond 30 days are increasingly in error due to the increasing degree of oxidation. One important measure for the conversion is the amount of bond scissions, which has been plotted in Figure 1 relative to the concentration of methyl groups, the latter being nearly the same as the concentration of chemical bonds in the system. The results indicate that the degradation rate achieves a steady state after about 15 days, when the radical and hydroperoxide concentrations achieve a constant value. Bond scissions dominate over crosslink formation, which leads to a decrease in the average molecular weight.  $M_w$  is estimated using the values of S and X using a relation reported in Mikdam et al. (2017):

$$M_w = \frac{2M_{w0}}{2 + (S - 4X)M_{w0}}$$

It should be noted that the results on S, X,  $[C=O]$  and  $M_w$  are sensitive to the choice of the rate constant  $k_{63}$ , since reactions (6-1) and (6-3) compete. For Figure 1, we chose to use the parameters from Colin et al. (2009), as the S/X ratio becomes close to the 5:1 ratio reported in Fayolle et al. (2007) for PE thermal degradation at 80-90 °C.

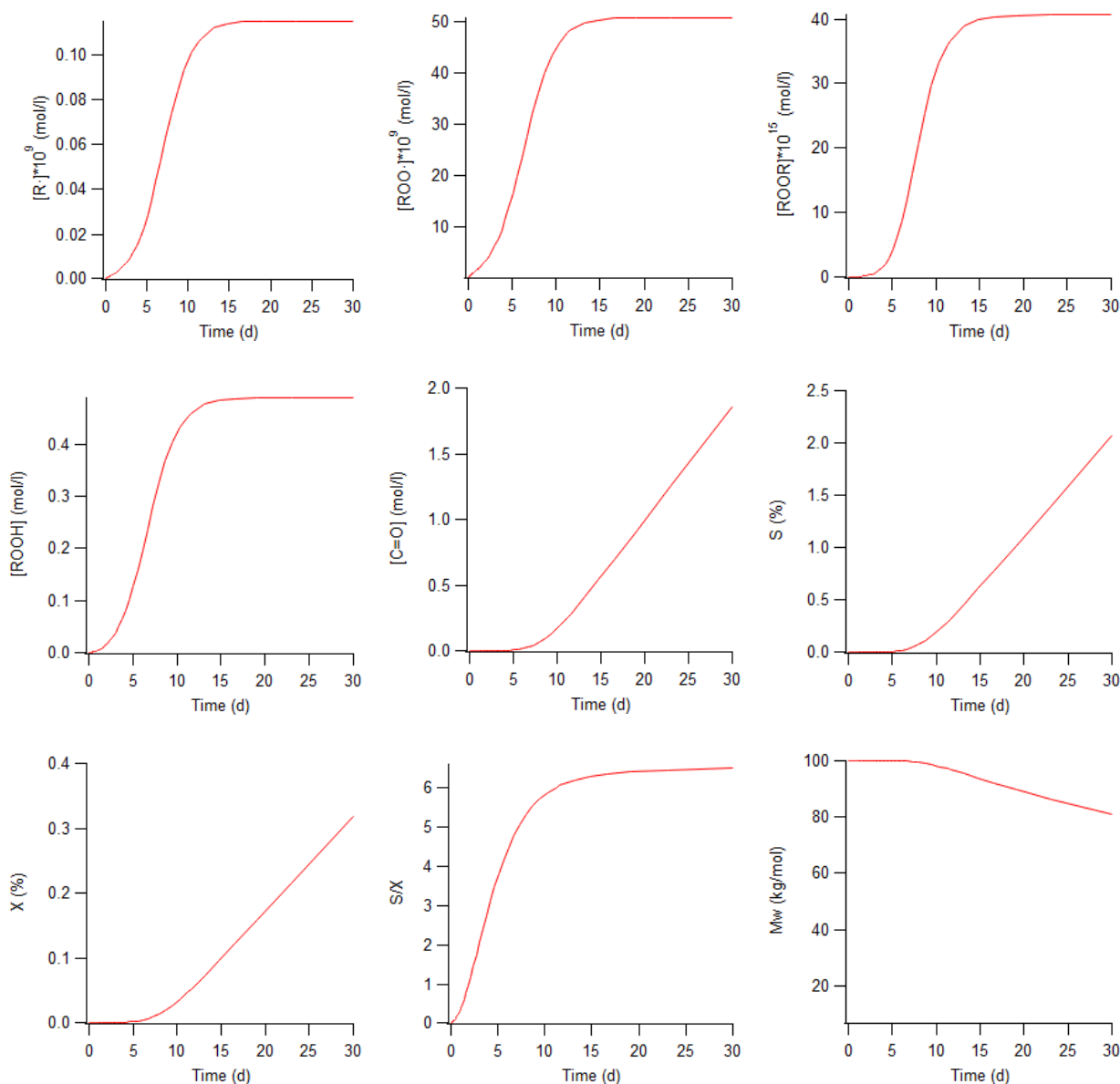


Figure 1. Time evolution of various species, bond scissions, crosslinks, and the average molecular weight during thermal ageing of linear PE at  $T=100$  °C.

### 3. Antioxidants

Antioxidants, also called heat stabilizers, are substances that suppress the thermal oxidation reactions resulting in chain scissions both in the processing stage and during service. They are divided into primary and secondary antioxidants (Tolinski 2015).

#### 3.1 Primary antioxidants

Primary antioxidants are also known as radical scavengers. They function by donating hydrogen to a free radical in a chain termination reaction. Thereby the antioxidant molecules become radicals themselves. However, the special chemical structure prevents these radicals from reacting further with polymers. Primary antioxidants are often hindered phenols, meaning that due to steric effects, the reactive site cannot

be readily accessed, and the radicalized molecule remains inactive. Also hindered amines and lactones can be used.

### 3.1.1 Phenolic antioxidants

In order to better understand the chemical action of primary antioxidants, it is instructive to start from the basic building block of phenolic antioxidants, the phenol molecule (Figure 1). It consists of a phenyl group  $C_6H_5$ , essentially a benzene ring minus one hydrogen, attached to a hydroxyl group. In Figure 2, the aromatic ring is displayed as alternating single and double bonds (the Kekulé structure), but in reality, the electrons in the  $\pi$ -orbitals are delocalized, forming a continuous band around the ring. The hydrogen of the hydroxyl group is not pointing radially away from the ring, but rather sits at an angle. This is due to the oxygen which has six electrons in its valence band. Two of them participate in chemical bonds, but the remaining two lone pairs need space to accommodate themselves, thus the C-O-H bond angle arises. This is also the reason for the H-O-H-angle in a water molecule. Phenol is slightly acidic, and in fact, it was originally called carbolic acid. This means that it is prone to donate a proton, specifically, the proton of the hydroxyl group. This property is the key to the antioxidant function of phenolic compounds, and any primary antioxidants, but it needs to be enhanced to make the antioxidant truly effective. Properties of the aromatic ring make such modifications quite feasible synthetically. However, we shall find out below that also natural evolution has produced effective phenolic antioxidants.

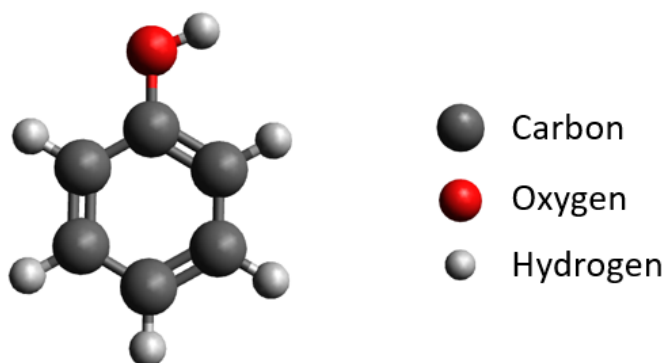


Figure 2. Structure of the phenol molecule.

The effectiveness of a primary antioxidant depends on the ease of which the hydroxyl group releases the proton, i.e. the hydroxyl bond dissociation energy, BDE(O-H). For phenol, this is about 370 kJ/mol (Lucarini et al. 1996). It turns out that modifying the structure of the aromatic ring by substituting the hydrogens by other groups, leads to changes in BDE. Viglianisi and Meninghetti (2019) explain this as follows. Despite being able to donate a proton, the hydroxyl group of phenol is an electron-donating (ED) group due to the presence of the oxygen lone pair electrons. In fact, parts of these delocalize in phenol by participating in the  $\pi$ -orbital of the ring. But when the hydroxyl group donates the proton, the resulting  $O^{\cdot-}$  radical becomes electron withdrawing (EW) (Lee and Grabowski 1992). Similarly, any substituent group can be viewed as either ED or EW. A combination of ED and EW groups increases the stability of the compound, while the presence of two or more similar groups decrease stability. It follows that if ED substitutive groups are added to the phenol ring, the stability of the phenol decreases, and the stability of the corresponding phenoxy radical increases.

One possibility to modify the phenol ring is to introduce alkyl group substitutes, e.g. a methyl group, (-CH<sub>3</sub>). In a methyl group, carbon is more electronegative than hydrogen, thereby drawing electron density from hydrogens towards carbon. In addition, the carbon has one lone electron pair which is subsequently pushed away from carbon. These factors make the methyl group an ED group, although relatively weakly. A more complex substituent is the tert-butyl group (-C-(CH<sub>3</sub>)<sub>3</sub>), which is also a slightly more effective ED.

However, due to the larger physical size, the tert-butyl group may introduce another important effect, *steric hindrance*. Figure 3 displays the structure of a 2,6 di-tert-butylphenol molecule. The tert-butyl groups together with the aromatic ring form a pocket surrounding the hydroxyl group. This makes the hydroxyl group less accessible to other molecules or radicals. More importantly, however, once the hydroxyl group has donated the proton, the remaining oxygen radical is even better shielded. Provided that the radical is suitably stabilized by the ED groups attached to the ring, it will not readily participate in reactions.

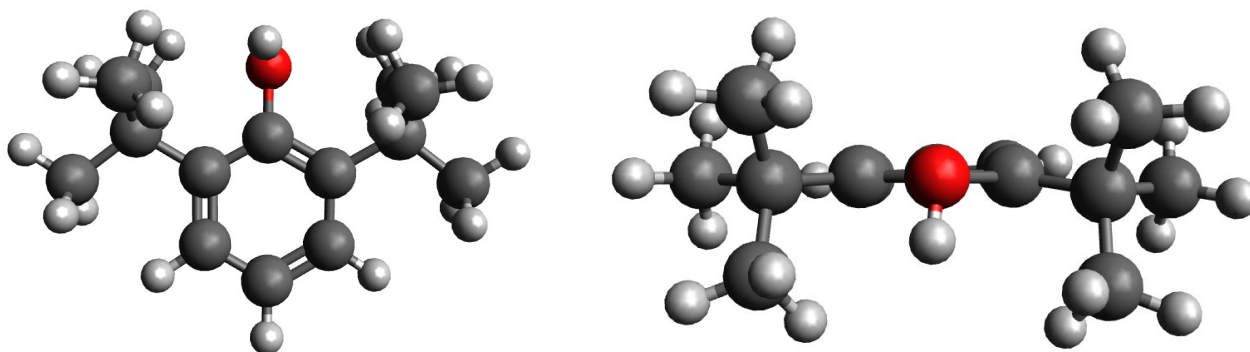
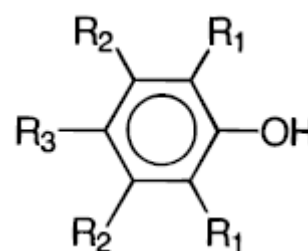


Figure 3. Structure of the 2,6 di-tert-butylphenol molecule. Left: side view. Right: top view.

Table 2. Experimentally determined O-H bond dissociation energies of substituted phenols. Adapted from (Lucarini et al.1996). Me = methyl group, CMe<sub>3</sub> = tert-butyl group, OMe = methoxy group.

R <sub>1</sub>	R <sub>2</sub>	R <sub>3</sub>	BDE (kJ/mol)
H	H	H	370 ± 3
H	H	Me	361 ± 3
H	H	CMe <sub>3</sub>	357 ± 2
H	H	OMe	347 ± 1
Me	H	H	354 ± 2
CMe <sub>3</sub>	H	H	347 ± 1
OMe	H	H	348 ± 1
H	CMe <sub>3</sub>	H	363 ± 1
H	OMe	H	363 ± 1
Me	H	Me	347 ± 1
CMe <sub>3</sub>	H	CMe <sub>3</sub>	340
OMe	H	OMe	335 ± 1
CMe <sub>3</sub>	H	Me	339 ± 1
CMe <sub>3</sub>	H	OMe	328 ± 1
Me	H, Me	OMe	332 ± 1
Me	Me	OMe	343 ± 1
HPMC			328 ± 1
α-tocopherol			328 ± 1



The effect of different substituents on the BDE in phenol is illustrated by the data in Table 2. The data shows that BDE is lowered by increasing the number of substitutions and that the efficiency of the

**beyond the obvious**

substituents increases in the order  $\text{Me} < \text{CMe}_3 < \text{OMe}$ . The position (ortho/meta/para) of the substituent also matters. An OMe substituent at the para position ( $\text{R}_3$ ) yields the lowest BDE values. The BDE for 2,6 di-tert-butylphenol is 347 kJ/mol.

The last two rows of Table 2 contain two non-phenolic substances, whose structures are shown in Figure 4. HPMC (6-hydroxy-2,2,5,7,8-pentamethylchroman) resembles a substituted phenol, but it is a heterocyclic compound belonging to the group of chromans where an aromatic ring is fused with a pyran ring. In addition to three alkyl groups in the phenol ring, this arrangement contains an oxygen atom in *para* position with respect to the hydroxyl group, but the pyran ring also induces other more subtle electronic effects lowering BDE. The second compound,  $\alpha$ -tocopherol, is essentially HPMC fitted with a hydrocarbon tail. It is also known as one possible form of vitamin E. This naturally occurring molecule combines the high antioxidant efficiency of HPMC with good solubility in fat, the latter caused by the hydrocarbon tail.

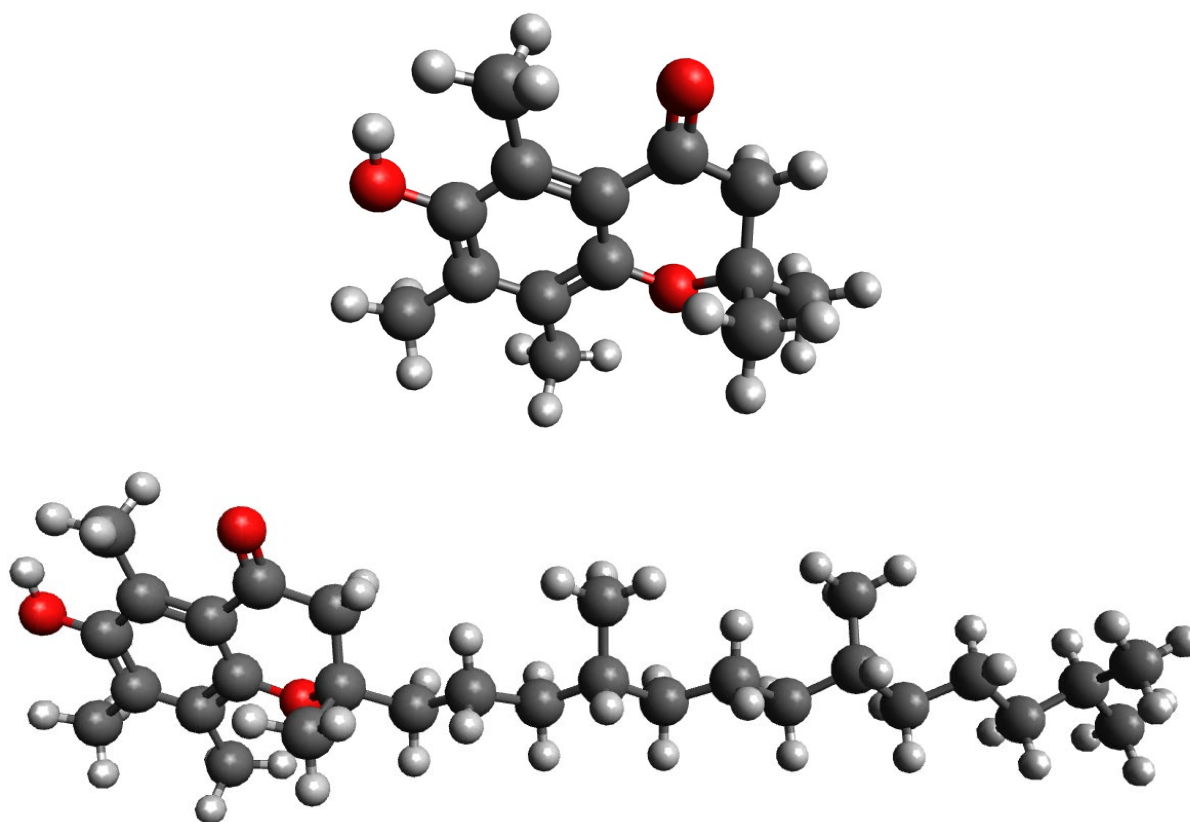


Figure 4. Top: 6-hydroxy-2,2,5,7,8-pentamethylchroman (HPMC). Bottom:  $\alpha$ -tocopherol (vitamin E).

The structure of two commercially used antioxidants, BHT (butylated hydroxytoluene) and Irganox 1076 are shown in Figure 5. Obviously, BHT is just 2,6 di-tert-butylphenol molecule appearing in Figure 3, but with an additional methyl group in the *para* position. BHT has been used widely in petroleum products and rubber, but it is especially popular as an additive for food and food packaging (Yehye et al. 2015). Irganox 1076 is also based on 2,6 di-tert-butylphenol, but it has a hydrocarbon tail attached to it via an ester bridge. Similarly to vitamin E, the tail provides solubility in hydrocarbons, and accordingly, Irganox 1076 is widely used for the protection of various plastics. Both BHT and Irganox 1076 are used at typical dosages of around 0.2 wt-% in their respective applications-

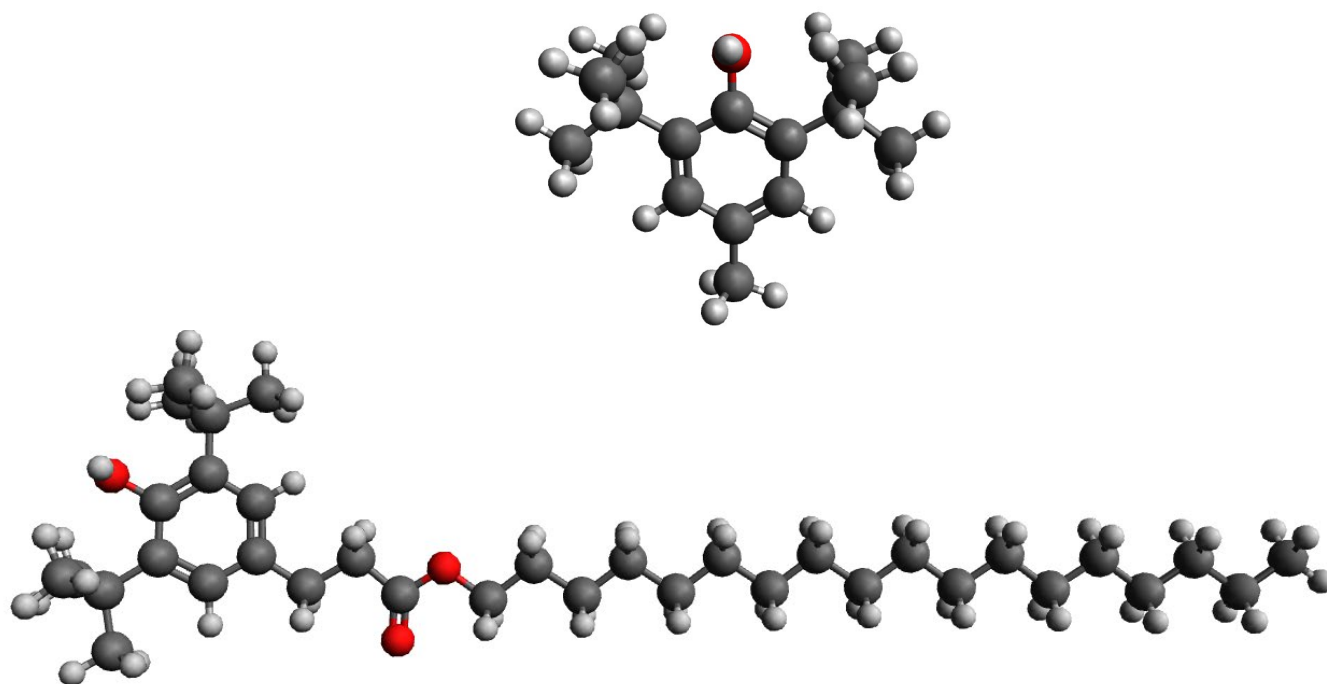


Figure 5. Top: butylhydroxytoluene (BHT). Bottom: Irganox 1076.

Another naturally occurring antioxidant is worth mentioning: lignin. It is the most abundant phenolic polymer on earth. Its chemical structure has different crosslinked phenolic structures, bonded together by ether linkages and carbonic structures. The guaiacyl and syringyl phenolic units of lignin are responsible for its antioxidant activity (Guilhen et al. 2017). The effectiveness of lignin as a primary antioxidant for synthetic polymer has been demonstrated (Gadioli et al. 2016).

### 3.1.2 Secondary aromatic amines

In addition to phenolic antioxidants, another important group of primary antioxidants are secondary aromatic amines. The simplest secondary aromatic amine, N-methylaniline, is shown in Figure 6, left. The molecule shown in Figure 6, right, is diphenylamine. Many commercial antioxidants (e. g. Naugard 445) are built around the diphenylamine structure. In secondary amines, the N-H bond of the amine group works much like the O-H bond of the phenolic hydroxyl group, i.e. by donating the hydrogen to a peroxy radical. After that, the chemistry of amines is more complex, which makes amines more effective than phenols. However, their transformation products (species formed during reactions) contain quinone mono- or diimines which absorb light in the visible wavelength region, and thus they cause discoloring (Pospisil et al. 2001).

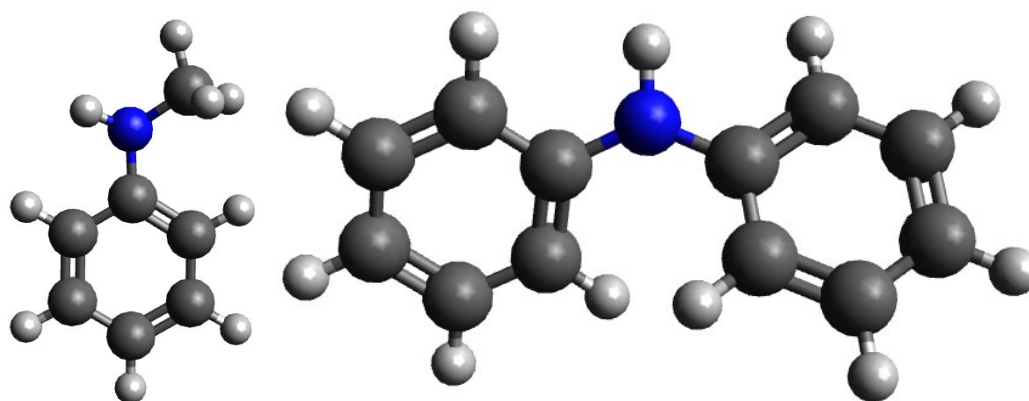


Figure 6. Left: *N*-methylaniline. Right: diphenylamine. The blue spheres represent nitrogen atoms.

### 3.1.3 Hindered amine light stabilizers

Hindered Amine Light Stabilizers (HALS) are structurally much like hindered phenols. However, they involve a piperidine ring as the basic structural unit, and often HALS compounds are derivatives of tetramethylpiperidine (Figure 7, left). Upon reaction with a peroxy, the amino group is converted to a nitroxide. The radical species in Figure 7, right, has a systematic name (2,2,6,6-tetramethylpiperidin-1-yl)oxyl, but it is commonly known as TEMPO, and it has a range of applications in chemistry and biochemistry. HALS compounds are used primary for UV protection of plastics, as they are not very effective in high processing temperatures. As UV protecting agents, they do not directly absorb UV, but react with the radical species of the oxidative degradation cycle. A particular feature of HALS compounds is that they are not consumed by the reactions, but are catalytically regenerated in a so-called Denisov cycle (Hodgson and Coote 2010).

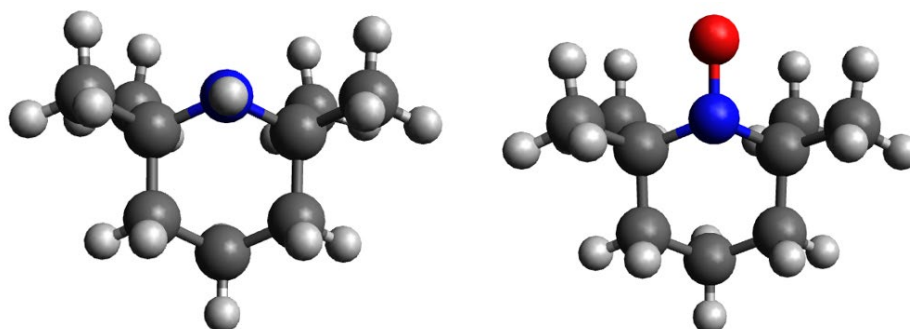


Figure 7. Left: tetramethylpiperidine. Right: 2,2,6,6-tetramethylpiperidin-1-yl)oxyl (TEMPO).

## 3.2 Secondary antioxidants

Secondary antioxidants are called peroxide decomposers. They react with hydroperoxides, converting them to alcohols, thereby preventing the hydroperoxide decomposition into free radicals. Secondary antioxidants are often used in conjunction with primary antioxidants, which reduces the consumption of the primary antioxidant. The most common secondary antioxidants are phosphites or sulfides. In these compounds, the functional groups are the phosphorus or sulfur atoms, which use their lone electron pairs for reactions with surrounding hydroperoxides. Two common secondary antioxidants are tris(nonylphenyl) phosphite (TNPP), and distearyl thio dipropionate (DSTDP or Irganox PS802), shown in Figure 8.

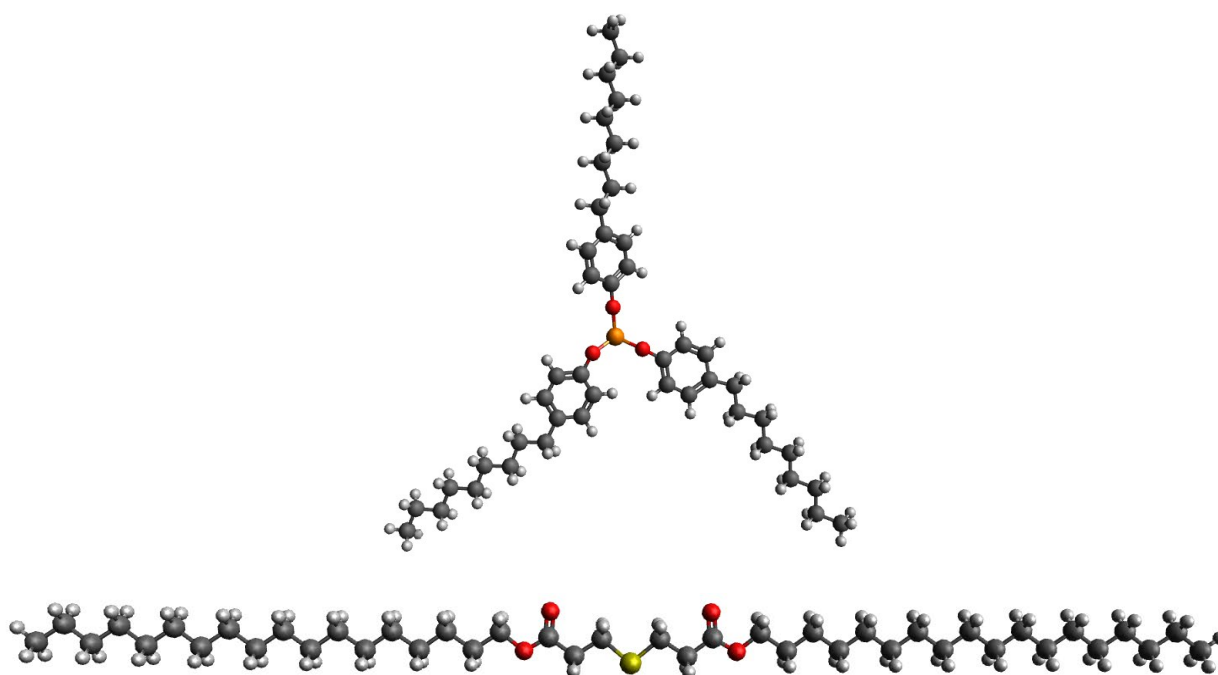


Figure 8. Top: tris(nonylphenyl) phosphite (TNPP). Bottom: distearyl thio dipropionate (DSTDP).

### 3.3 Multi-functional antioxidants

It is also possible to synthesize molecules that combine the functionalities of primary and secondary antioxidants in the same molecule. Such molecules are called multi-functional antioxidants. An example is 6,6'-di-tert-butyl-4,4'-thiodi-m-cresol (Figure 9), where two primary phenolic antioxidant groups are joined by a sulfur bridge which provides the secondary antioxidant function.

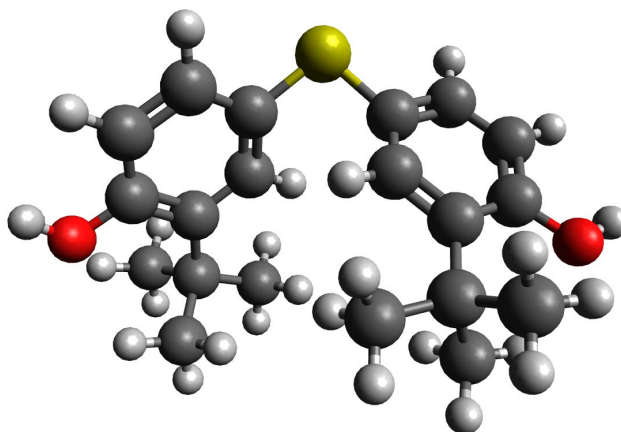


Figure 9. 6,6'-di-tert-butyl-4,4'-thiodi-m-cresol.

### 3.4 Physical properties of antioxidants

While the main purpose of this report is to present the chemistry and chemical kinetics of antioxidants, it is nonetheless important to understand that there are other aspects that are vitally important for antioxidant performance and which may therefore limit the usefulness of pure chemical kinetics considerations. These



are physical loss, solubility and mobility (Boersma 2006). Loss of antioxidant through evaporation or leaching is in most cases more significant than loss due to chemical reactivity (Allen et al. 2010).

That an antioxidant can be physically lost from the material requires diffusive transport of the antioxidant molecules from the bulk to the surface. The most important property of an antioxidant molecule with respect to diffusion is the molecular weight (i.e. physical size), because diffusion in the polymer matrix is defined by the fluctuating free volume available for the molecule to move about (Ramesh et al. 2011). Often the apparent structural complexity of antioxidant molecules follows from an attempt to design a certain molecular weight.

Small molecular weight for the antioxidant means that molecules have large diffusion coefficients. This is advantageous if one considers reactivity: chemical reaction rates are essentially proportional to collision rates between reactants, and fast diffusion means more collisions. Fast diffusion also ensures the homogeneous distribution of the antioxidant. The downside is that small molecules (such as BHT) are also effectively transported from bulk to surface, which promotes physical loss, especially at processing temperatures or elevated service temperatures. Increasing molecular weight slows down both diffusion and physical loss, and choosing an optimal molecular weight is a non-trivial problem, interconnected with the number of functional groups per molecule.

However, there appears to be an upper limit for effective molecular weight. Analysis by Gugumus (2000) for HALS compounds in polypropylene suggests decreasing effectiveness above the molecular weight of 1000 g/mol, which is mainly attributed to decreasing compatibility between a large additive molecule and the polymer matrix. For very large molecular weights (above 10000 g/mol) also the dimensions of the amorphous domains become an issue. Beer et al. (2014) discuss special techniques to reduce antioxidant mobility, including grafting of antioxidants to polymers or additive minerals, or co-polymerization of antioxidant-containing monomers with the base polymer. However, such techniques can be difficult and/or expensive.

Besides molecular weight, another important reason for adding structural elements to functional groups is solubility. As discussed in connection with vitamin E and Irganox 1076, a hydrocarbon tail gives these molecules either solubility in fat or compatibility with a synthetic polymer, in the spirit of the empirical “like dissolves like” rule. A more formal, yet empirical statement of this principle is provided by Hansen solubility parameters (Hansen 2004, Hansen 2007). Each molecule is given three parameters:

- $\delta_D$ : energy from nonpolar (dispersion) forces between molecules
- $\delta_P$ : energy from dipolar forces between molecules
- $\delta_H$ : energy from hydrogen bonds between molecules

For a combination of two substances, such as additive and polymer, a distance in the Hansen space is calculated as

$$R_a = \sqrt{4(\delta_{D2} - \delta_{D1})^2 + (\delta_{P2} - \delta_{P1})^2 + (\delta_{H2} - \delta_{H1})^2}$$

One then defines a distance  $R_0$  to compute a relative energy difference  $RED=R_a/R_0$  such that

- $RED < 1$ : molecules will dissolve
- $RED = 1$ : molecules will partially dissolve
- $RED > 1$ : molecules will not dissolve

In practice, values for  $\delta_D$ ,  $\delta_P$ ,  $\delta_H$  and  $R_0$  will need to be determined experimentally (Gharagheizi 2007).

Antioxidants may be present in the polymer in concentrations above the solubility limit. In this case, the excess antioxidant forms a dispersed phase, and in the case of semicrystalline polymers is located mainly in interfibrillar zones of spherulite and in gaps between spherulites (Lin and Vorob'eva 2017). The rest

remains dissolved in the amorphous phase. When antioxidant is consumed from the amorphous phase, the dispersed phase will release additional antioxidant, acting as a reserve.

The kinetic modelling in this report implicitly assumes that the antioxidant as well as other reacting species are always homogeneously distributed. This may however not always be the case, as suggested by a study on the stabilization of a polybutadiene elastomer by a phenolic antioxidant (Celina et al. 2006). In particular, loss of mechanical properties and signs of oxidative degradation were observed at low temperatures despite significant levels of free antioxidant in the material. This was attributed either to an ineffective antioxidant or just a fraction of the antioxidant actually involved in the inhibition process. Further literature search on this issue would be warranted.

## 4. Reaction kinetics of antioxidants

### 4.1 Reaction mechanisms

As mentioned above in 3.1.1, the key property of phenolic antioxidants is the donation of the proton from the hydroxyl group. Specifically, the hydroxyl group reacts with a peroxy radical to form a hydroperoxide. However, the resulting antioxidant radical is able to further react with another radical species to form a stable product. This scheme is illustrated in Figure 10 for BHT (Kuzema et al. 2015):

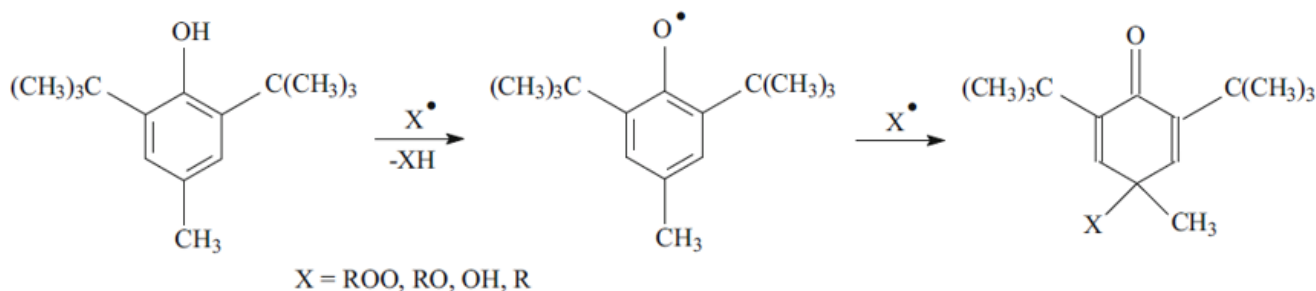


Figure 10. Reaction mechanism for BHT antioxidant.

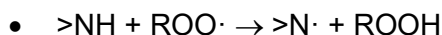
Thus, when modelling kinetics of primary antioxidants, the following reaction equations should be added to the oxidative degradation mechanism (Richaud 2013):

- $\text{AH} + \text{ROO}\cdot \rightarrow \text{A}\cdot + \text{ROOH}$  (S1)
- $\text{A}\cdot + \text{ROO}\cdot \rightarrow \text{ROOA}$  (S2)

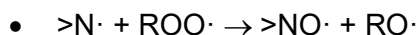
where A stands for the antioxidant molecule, and A· for the corresponding radical. Note that according to Figure X there could be reactions involving other species than peroxy radicals. However, Richaud et al. (2011) have concluded that including reactions (S1) and (S2) is sufficient.

From the basic oxidative reaction scheme, it can be observed that these reactions are in competition with propagation reaction (3). As pointed out by (Huang et al. 2021), if no antioxidants are present, reaction (3) consumes one ROO· radical and produces 3 radicals (R·, RO· and OH·), since hydroperoxides decompose into RO· and OH· radicals. If antioxidants are present, and if the rate constants are such that  $k_3 \ll k_{S1}$ , reactions (S1) and (S2) consume 2 ROO· radicals and produce 2 radicals (RO· and OH·). This is the kinetic reason for the effectiveness of phenols, but it requires making hydrogen donation from the hydroxyl group as easy as possible.

The detailed transformation chemistry of both aromatic amines and hindered amine light stabilizers is considerably more complex than that of phenols and is beyond the scope of this report (Jensen et al. 1995, Pospisil et al. 2001, Hodgson and Coote 2010, Soleimani et al. 2018). Here, it suffices to say that for both classes of antioxidants, the first step involves the reaction of the amine group with an alkoxy or peroxy radicals



followed by a further reaction with the same radicals



yielding a nitroxide radical which participates in further reactions that are either sacrificial (consuming the reactant) or regenerative, or a mix of both, depending on the compound, temperature, etc.

On the contrary, reaction mechanisms for secondary antioxidants are straightforward (Figure 11). A typical phosphorus-based secondary antioxidant is trivalent phosphite. This leaves one lone pair of electrons for the phosphorus, which readily reacts with a hydroperoxide to convert the latter to alcohol which is an inactive species with respect to polymer oxidation. Sulfides are typically divalent sulfur compounds, leaving two lone pairs for the sulfur to react with two hydroperoxide molecules, again producing alcohols.

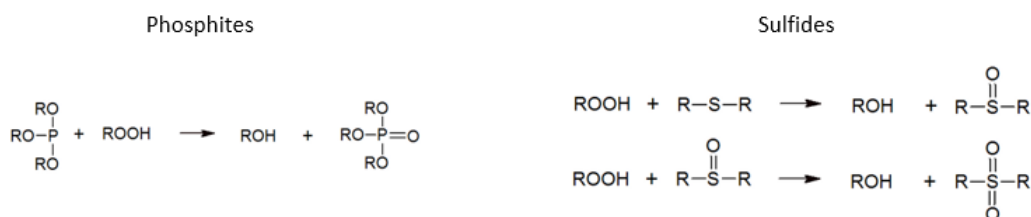


Figure 11. Reaction mechanisms for secondary antioxidants.

## 4.2 Kinetic modelling of phenolic antioxidants

In this report, we demonstrate kinetic modelling of primary phenolic antioxidants, noting that an example of kinetic modelling of HALS compounds is found in (Huang et al. 2021) and the much simpler case of secondary antioxidant kinetics is treated by (Xu et al. 2020b). Equations (S1) and (S2) require introducing additional equations and terms to the system of differential equations, which becomes

$$\frac{d[R\cdot]}{dt} = G \cdot 10^{-7} \cdot I + 2k_{1u}[ROOH] + k_{1b}[ROOH]^2 - k_2[O_2][R\cdot] + k_3[ROO\cdot][RH] - 2k_4[R\cdot]^2 - k_5[R\cdot][ROO\cdot] + 2k_{63}[ROOR]_{cage}$$

$$\frac{d[ROO\cdot]}{dt} = k_{1b}[ROOH]^2 + k_2[O_2][R\cdot] - k_3[ROO\cdot][RH] - 2k_4[R\cdot]^2 - k_5[R\cdot][ROO\cdot] + 2k_{60}[ROO\cdot]^2 - k_{S1}[ROO\cdot][AH] - k_{S2}[ROO\cdot][R\cdot]$$

$$\frac{d[ROOH]}{dt} = -k_{1u}[ROOH] - 2k_{1b}[ROOH]^2 + k_3[ROO\cdot][RH] - 2k_4[R\cdot]^2 - k_5[R\cdot][ROO\cdot] + k_{S1}[ROO\cdot][AH]$$

$$\frac{d[ROOR]_{cage}}{dt} = k_{60}[ROO\cdot]^2 - (k_{61} + k_{62} + k_{63})[ROOR]_{cage}$$

$$\frac{d[O_2]}{dt} = -k_2[O_2][R \cdot] + 2k_{60}[ROO \cdot]^2$$

$$\frac{d[AH]}{dt} = -k_{S1}[ROO \cdot][AH]$$

$$\frac{d[A \cdot]}{dt} = k_{S1}[ROO \cdot][AH] - k_{S2}[ROO \cdot][A \cdot]$$

For the rate constant  $k_{S1}$ , Richaud (2013) reports a pre-exponential factor of  $2.0 \cdot 10^{16}$  l/mol/s, and activation energy of 86.7 kJ/mol. It is readily verified that  $k_3 \ll k_{S1}$  for temperatures of interest. For  $k_{S2}$ , a value of  $5.0 \cdot 10^8$  l/mol/s is used regardless of temperature.

The effectiveness of an antioxidant system can be measured by heating a sample in a DSC apparatus under an inert atmosphere. Oxygen is then introduced, and the time is measured to the point when DSC starts to show endothermic events in the sample. The time is called Oxidation Induction Time (OIT). Let us first apply the kinetic model to study the relationship between antioxidant concentration and OIT. Figure 12 (left) displays the time evolution of antioxidant concentration at a temperature of 200 °C for four different initial concentrations. The OIT is taken as the point at which the antioxidant concentration drops to zero. The right-hand side of Figure 12 shows the OIT as a function of antioxidant concentration. The dependence is nearly linear.

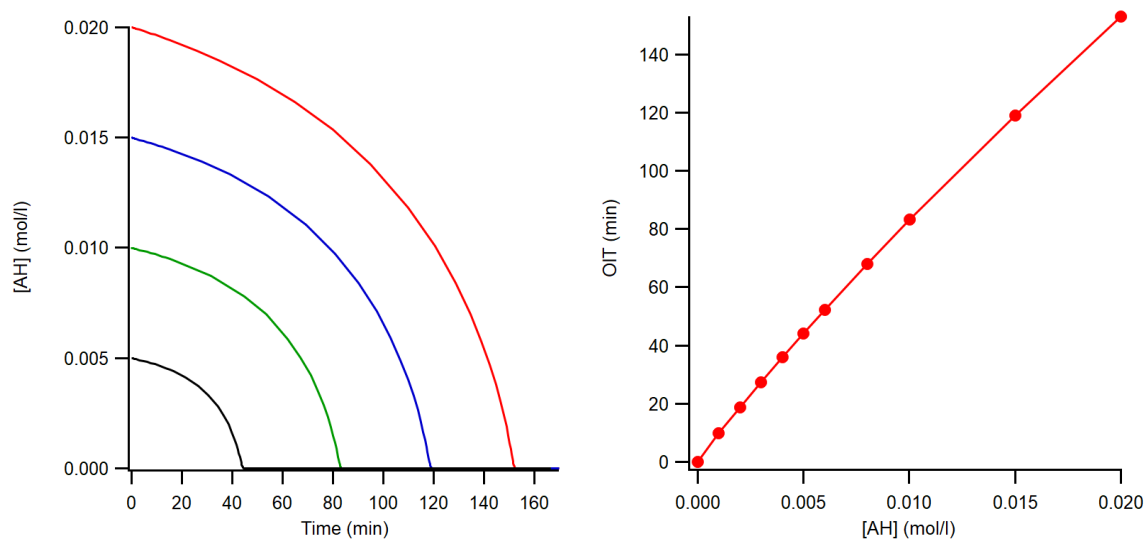


Figure 12. Left: time evolution of antioxidant concentration at 200 °C. Right: oxidation induction time as a function of antioxidant concentration.

Antioxidant dosages in real materials are normally given in wt-%. Relating the molar antioxidant concentration to the mass concentration requires therefore knowledge of the molar mass  $M_{AH}$  of the antioxidant. That is not all, however. First,  $[AH]$  in the kinetic model is the molar concentration of the functional groups of the antioxidants. In Irganox 1076, there is one hydroxyl group per molecule, but in Irganox 1010 there are four. We note the number of functional groups per molecule by  $f_{AH}$ . In addition, in a semicrystalline material, the antioxidant exists only in the amorphous phase, whereas the concentration is given for the entire material. Denoting the crystallinity by  $X_C$ , the antioxidant molar concentration is given by (Richaud 2013)

$$[AH] = \frac{1}{1 - X_C} \frac{\rho_P}{M_{AH}} x_{AH} f_{AH}$$



where  $\rho_P$  is the density of the polymer and  $x_{AH}$  is the weight fraction of antioxidant. Consider for example polyethylene for which  $\rho_P=935 \text{ kg/m}^3$  and  $X_C=0.5$ . Irganox 1076 has a molar mass of 0.531 kg/mol and  $f_{AH}=1$ . Irganox 1010 has a molar mass of 1.18 kg/mol and  $f_{AH}=4$ . Therefore,

- $[\text{Irganox 1076}] = 3.5 \text{ mol/l} * x_{\text{Irganox 1076}}$
- $[\text{Irganox 1010}] = 6.3 \text{ mol/l} * x_{\text{Irganox 1010}}$

For Irganox 1076 in XLPE, Xu et al. (2020a) have determined a solubility of 0.016 mol/l (0.46 wt-%). Concentrations above that lead to presence of a dispersed crystalline antioxidant phase which acts as a reservoir when the antioxidant in the amorphous phase is depleted.

Consider now accelerated ageing of antioxidant containing polyethylene, assuming an initial antioxidant concentration of 0.02 mol/l. Figure 13 (top left) displays the ageing time required to completely deplete the antioxidant as a function of temperature for purely thermal ageing and two radiation dose rates. The plot for purely thermal ageing on a logarithmic scale is linear, reflecting the Arrhenius kinetics associated with most reaction rates. However, for radiative cases the behaviour of the data changes, with the dependence on temperature becoming weaker as the temperature is lowered. This is the result of the dominance of the radiative term in the initiation reactions, which is independent of temperature. The dominance of radiation is also reflected in a significant reduction in the time required to deplete the antioxidant.

Using the kinetic model, it is instructive to check how the remaining OIT correlates with the antioxidant concentration, given the nearly-linear dependence shown above for fresh material. In order to do this, the concentrations of all species are recorded at a selected time during the ageing, and they are used as initial values for an OIT simulation corresponding to that ageing duration. The result is shown in Figure 13 (top right), which assumes purely thermal ageing at 100 °C, and an initial antioxidant concentration of 0.02 mol/l. Ageing drastically alters the OIT vs [AH] plot compared to the fresh material, and the reason is that the simulation is highly sensitive to the initial concentration of hydroperoxides, at least using the kinetic parameters of Table 1.

Finally, the OIT vs ageing time is displayed in Figure 13, bottom. It is seen that estimating the remaining lifetime based on the value of OIT is not trivial and may result in a large error. In particular, OIT values around 10% of the initial OIT do not necessarily mean that the cable has either reached or is about to reach the end of its lifetime. In this context it can be noted that in many studies an exponential dependence of OIT on time is assumed:

$$OIT = OIT_0 e^{-st}$$

where  $s$  is a constant antioxidant depletion rate determined from an Arrhenius plot (see e.g. Li et al. 2021). However, the kinetic model does not predict an [AH] depletion rate proportional to its concentration (see Figure 12), and accordingly, an exponential fit to the OIT(t) predicted by the kinetic model is not satisfactory.

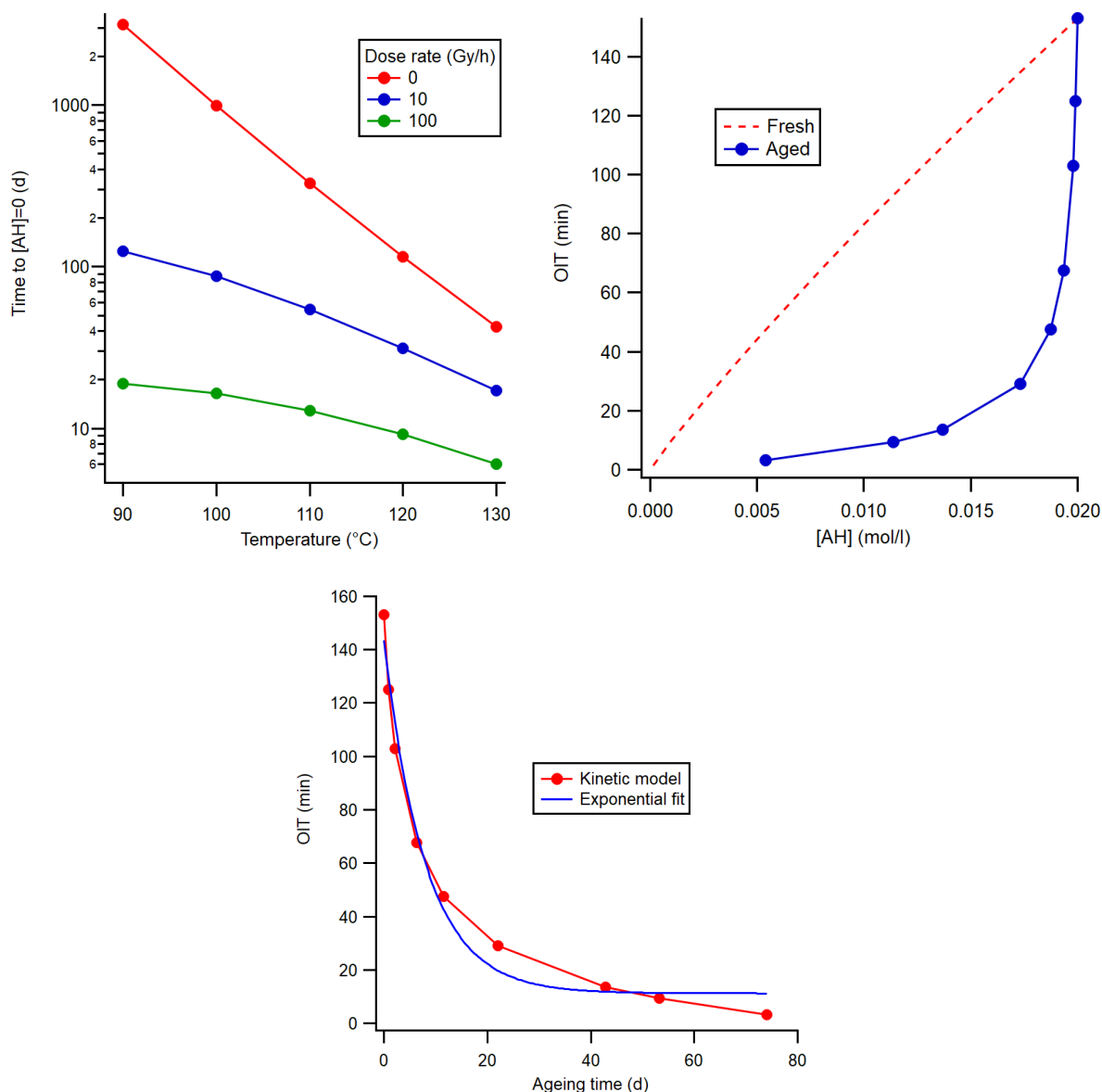


Figure 13. Top left: antioxidant depletion time at various temperatures and dose rates. Top right: oxidation induction time as a function of antioxidant concentration for fresh and aged materials. Bottom: oxidation induction time as a function of ageing time.

## 5. Summary

This report has presented a literature survey on antioxidants intended to provide protection against oxidative degradation of polyolefin materials, and in particular, the reaction kinetics involved. Since antioxidants are designed to react with the intermediate products of the polyolefin degradation reaction rather than oxygen, an introduction to the oxidative degradation kinetics of unstabilized polyolefin materials was first given. A kinetic model describing oxidative degradation of pure polymer material was presented, and an example simulation on thermal ageing was conducted.

This was followed by an introduction of the main types of antioxidants, with the main focus on their chemical structure and reactivity, but also information on their physical properties. Subsequently, equations describing the inhibiting action of antioxidants were introduced into the kinetic model. The model was used



to simulate the oxidative induction time experiment of both fresh and aged materials, as well as thermal and thermo-radiative ageing of materials.

The main assumptions of the kinetic model presented in this report were oxygen excess and homogeneous distribution of reacting species. Effects arising from transport limitations were excluded, but need to be included in further work. A particular issue requiring further work is related to possible chemical ineffectiveness and/or transport limitations of antioxidants, which could lead to oxidative degradation despite significant levels of antioxidant remaining in the material.

## References

---

- Ahmad, I., Li, C.Y., Hsuan, Y.G., Cairncross, R.A. 2014. Reaction model describing antioxidant depletion in polyethylene-clay nanocomposites under thermal aging. *Polymer Degradation and Stability* vol. 110 pp. 318-335. <http://dx.doi.org/10.1016/j.polymdegradstab.2014.09.002>
- Allen, N.S., Zeynalov, E.B., del Teso Sanchez, K., Edge, M., Kabetkina, Y.P., Johnson, B. 2010. Comparative Evaluation of the Efficiency of a Series of Commercial Antioxidants Studied by Kinetic Modeling in a Liquid Phase and During the Melt Processing of Different Polyethylenes. *Journal of Vinyl & Additive Technology* vol. 16 pp. 1-14. <https://doi.org/10.1002/vnl.20208>
- Boersma, A. 2006. Predicting the efficiency of antioxidants in polymers. *Polymer Degradation and Stability* vol. 91 pp. 472-478. <https://doi.org/10.1016/j.polymdegradstab.2005.08.007>
- Borden, W.T., Hoffmann, R., Stuyver, T. and Chen, B. 2017. Dioxygen: What Makes This Triplet Diradical Kinetically Persistent? *Journal of the American Chemical Society* vol. 139 pp. 9010-9018. <https://doi.org/10.1021/jacs.7b04232>
- Braden, D.A., Parrack, E.E. and Tyler, D.R. 2001. Solvent cage effects. I. Effect of radical mass and size on radical cage pair recombination efficiency. II. Is geminate recombination of polar radicals sensitive to solvent polarity? *Coordination Chemistry Reviews* vol. 211 pp. 279-294.
- Celina, M.C. 2013. Review of polymer oxidation and its relationship with materials performance and lifetime prediction. *Polymer Degradation and Stability* vol. 98 pp. 2419-2429. <http://dx.doi.org/10.1016/j.polymdegradstab.2013.06.024>
- Colin, X., Audouin, L., Verdu, J., Rozental-Evesque, M., Rabaud, B., Martin, F., Bourguine, F. 2009. Aging of Polyethylene Pipes Transporting Drinking Water Disinfected by Chlorine Dioxide. I. Chemical Aspects. *Polymer Engineering and Science* vol. 49 pp. 1429-1437. <https://doi.org/10.1002/pen.21258>
- Colin X., Verdu J. 2012. Mechanisms and Kinetics of Organic Matrix Thermal Oxidation. In: Pochiraju K., Tandon G., Schoeppner G. (eds) *Long-Term Durability of Polymeric Matrix Composites*. Springer, Boston, MA
- Fayolle, B., Colin, X., Audouin, L., Verdu, J. 2007. Mechanism of degradation induced embrittlement in polyethylene. *Polymer Degradation and Stability* vol. 92 pp. 231-238.
- Gadioli, R., Waldman W.R., De Paoli, M.A. 2016. Lignin as a green primary antioxidant for polypropylene. *Journal of Applied Polymer Science* vol. 133, 43558. <https://doi.org/10.1002/app.43558>
- Gharagheizi, F. 2007. New Procedure To Calculate the Hansen Solubility Parameters of Polymers. *Journal of Applied Polymer Science* vol.103 pp. 31-36. <https://doi.org/10.1002/app.23874>

- Gugumus, F. 2000. Aspects of the impact of stabilizer mass on performance in polymers 2. Effect of increasing molecular mass of polymeric HALS in PP. *Polymer Degradation and Stability* vol. 67 pp. 299-311. [https://doi.org/10.1016/S0141-3910\(99\)00131-7](https://doi.org/10.1016/S0141-3910(99)00131-7)
- Guilhen, A., Gadioli, R., Fernandes, F.C., Waldman, W.R., De Paoli, M.A. 2017. High-density green polyethylene biocomposite reinforced with cellulose fibers and using lignin as antioxidant. *Journal of Applied Polymer Science* vol. 134, 45219. <https://doi.org/10.1002/app.45219>
- Hansen, C.M. 2004. Polymer additives and solubility parameters. *Progress in Organic Coatings* vol. 51 pp. 109-112. <https://doi.org/10.1016/j.porgcoat.2004.05.003>
- Hansen, C.M. 2007. Hansen Solubility parameters. A User's handbook. 2<sup>nd</sup> Edition. CRC Press. <https://doi.org/10.1201/9781420006834>
- Hettal, S., Roland, S., Sipilä, K., Joki, H., Colin, X. 2021. A new analytical model for predicting the radio-thermal oxidation kinetics and the lifetime of electric cable insulation in nuclear power plants: application to silane cross-linked polyethylene. *Polymer Degradation and Stability* vol. 185, 109492. <https://doi.org/10.1016/j.polymdegradstab.2021.109492>
- Hodgson, J.L., Coote, M.L. 2010. Clarifying the Mechanism of the Denisov Cycle: How do Hindered Amine Light Stabilizers Protect Polymer Coatings from Photo-oxidative Degradation? *Macromolecules* vol. 43 pp. 4573-4583. <https://doi.org/10.1021/ma100453d>
- Jensen, R.K., Korcek, S., Zinbo, M., Gerlock, J.L. 1995. Regeneration of Amine in Catalytic Inhibition of Oxidation. *Journal of Organic Chemistry* vol. 60 pp. 5396-5400. <https://doi.org/10.1021/jo00122a014>
- Khelidj, N., Colin, X., Audouin, L., Verdu, J. 2005. A simplified approach for the lifetime prediction of PE in nuclear environments. *Nuclear Instruments and Methods in Physics Research B* vol. 236 pp. 88-94. <https://doi.org/10.1016/j.nimb.2005.03.259>
- Khelidj, N., Colin, X., Audouin, L., Verdu, J., Monchy-Leroy, C., Prunier, V. 2006. Oxidation of polyethylene under irradiation at low temperature and low dose rate. Part II. Low temperature thermal oxidation. *Polymer Degradation and Stability* vol. 91 pp. 1598-1605. <https://doi.org/10.1016/j.polymdegradstab.2005.09.012>
- Kuzema, P.O., Bolbukh, Yu.M., Tertykh, V.A., Laguta, I.V. 2015. Vacuum thermal decomposition of polyethylene containing antioxidant and hydrophilic/hydrophobic silica. *Journal of Thermal Analysis and Calorimetry* vol. 121 pp. 1167-1180. <https://doi.org/10.1007/s10973-015-4646-5>
- Lee, J., Grabowski, J.J. 1992. Reactions of the Atomic Oxygen Radical Anion and the Synthesis of Organic Reactive Intermediates. *Chemical Reviews* vol. 92 pp. 1611-1647.
- Li, W., Xu, Ya., Huang, Q., Liu, Y., Liu, J. 2021. Antioxidant depletion patterns of high-density polyethylene geomembranes in landfills under different exposure conditions. *Waste Management* vol. 121 pp. 365-372. <https://doi.org/10.1016/j.wasman.2020.12.025>
- Lin, D.G., Vorob'eva, E.V. 2017. Decrease in the Performance of a Phenolic Antioxidant in Preparation of Inhibited Polyethylene Films by Hot Pressing. *Russian Journal of Applied Chemistry* vol. 90 pp. 780-787. <https://doi.org/10.1134/S1070427217050196>
- Lucarini, M., Pedrielli, P., Pedulli, G.F., Cabiddu, S., Fattuoni, C. 1996. Bond Dissociation Energies of O-H Bonds in Substituted Phenols from Equilibration Studies. *The Journal of Organic Chemistry* vol. 61 pp. 9259-9263.



- Mikdam, A., Colin, X., Minard, G., Billon, N., Maurin, R. 2017. A kinetic model for predicting the oxidative degradation of additive free polyethylene in bleach desinfected water. *Polymer Degradation and Stability* vol. 146 pp. 78-94. <http://dx.doi.org/10.1016/j.polymdegradstab.2017.09.020>
- Pospisil, J., Habicher, W.-D., Al-Malaika, S., Zweifel, H., Nespres, S. 2001. Phenols and aromatic Amines as Thermal Stabilizers in Polyolefin Processing. *Macromolecular Symposia* vol. 176 pp. 55-63. [http://dx.doi.org/10.1002/1521-3900\(200112\)176:1%3C55::AID-MASY55%3E3.0.CO;2-H](http://dx.doi.org/10.1002/1521-3900(200112)176:1%3C55::AID-MASY55%3E3.0.CO;2-H)
- Ramesh, N., Davis, P.K., Zielinski, J.M., Danner, R.P., Duda, J.L. 2011. Application of Free-Volume Theory to Self Diffusion of Solvents in Polymers Below the Glass Transition Temperature: A Review. *Journal of Polymer Science Part B: Polymer Physics* vol. 49 pp. 1629-1644. <https://doi.org/10.1002/polb.22366>
- Richaud, E., Fayolle, B., Verdu, J. 2011. Polypropylene stabilization by hindered phenols - Kinetic aspects. *Polymer Degradation and Stability* vol. 96 pp. 1-11. <https://doi.org/10.1016/j.polymdegradstab.2010.11.011>
- Richaud, E. 2013. Kinetic modelling of phenols consumption during polyethylene thermal oxidation. *European Polymer Journal* vol. 49 pp. 2223-2232. <http://dx.doi.org/10.1016/j.eurpolymj.2013.04.027>
- Soleimani, M., Dehabadi, L., Wilson, L.D. and Tabil, L.G. 2018. Antioxidants Classification and Applications in Lubricants. In: "Tribology, Lubricants and Additives", Johnson, D.W. (ed.). IntechOpen. <https://doi.org/10.5772/intechopen.72621>
- Tolinski, M. 2015. Additives for Polyolefins - Getting the Most Out of Polypropylene, Polyethylene and TPO (2nd Edition). Elsevier. <https://app.knovel.com/hotlink/toc/id:kpAPGMOPP2/additives-polyolefins/additives-polyolefins>
- Verdu, J. 2013. Oxidative Ageing of Polymers. Online version. John Wiley & Sons, Inc. Online ISBN:9781118562598. <https://doi.org/10.1002/9781118562598>
- Viglianisi, C., Menichetti, S. 2019. Chain Breaking Antioxidant Activity of Heavy (S, Se, Te) Chalcogens Substituted Polyphenols. *Antioxidants* vol. 8, 487. <https://doi.org/10.3390/antiox8100487>
- Walling, C. and Padwa, A. 1963. Positive halogen compounds. VI. Effects of structure and medium on the  $\beta$ -scission of alkoxy radicals. *J. Am. Chem. Soc.* vol. 85 pp. 1593-1597.
- Yehye, W.A., Abdun Rahman, N., Ariffin, A., Bee Abd Hamid, S., Alhadi, A.A., Kadir, F.A., Yaeghoobi, M. 2015. Understanding the chemistry behind the antioxidant activities of butylated hydroxytoluene (BHT): A review. *European Journal of Medicinal Chemistry* vol. 101 pp. 295-312. <http://dx.doi.org/10.1016/j.ejmech.2015.06.026>
- Xu, A., Roland, S., Colin, X. 2020a. Physico-chemical characterization of the blooming of Irganox 1076® antioxidant onto the surface of a silane-crosslinked polyethylene. *Polymer Degradation and Stability* vol. 171, 109046. <https://doi.org/10.1016/j.polymdegradstab.2019.109046>
- Xu, A., Roland, S., Colin, X. 2020b. Thermal ageing of a silane-crosslinked polyethylene stabilised with a thiodipropionate antioxidant. *Polymer Degradation and Stability* vol. 181, 109276. <https://doi.org/10.1016/j.polymdegradstab.2020.109276>

**Certificate Of Completion**

Envelope Id: D026B8C0F01A4AE585C27C44DDA7561E	Status: Completed
Subject: Please Sign: VTT-R-01051-21.pdf	
Source Envelope:	
Document Pages: 25	Signatures: 1
Certificate Pages: 1	Initials: 0
AutoNav: Enabled	Envelope Originator:
Envelopeld Stamping: Enabled	Christina Vähävaara
Time Zone: (UTC+02:00) Helsinki, Kyiv, Riga, Sofia, Tallinn, Vilnius	Vuorimiehentie 3, Espoo, .. . P.O Box1000,FI-02044 Christina.Vahavaara@vtt.fi IP Address: 130.188.17.16

**Record Tracking**

Status: Original	Holder: Christina Vähävaara	Location: DocuSign
25 January 2022   14:50	Christina.Vahavaara@vtt.fi	

**Signer Events**

Mikko Vepsäläinen  
mikko.vepsalainen@vtt.fi  
Security Level: Email, Account Authentication  
(None), Authentication

**Signature**

DocuSigned by:  
  
F52E9E6DFBE54A1...

Signature Adoption: Pre-selected Style  
Using IP Address: 86.115.193.124

**Timestamp**

Sent: 25 January 2022 | 14:52  
Viewed: 25 January 2022 | 17:24  
Signed: 25 January 2022 | 17:25

**Authentication Details**

SMS Auth:  
Transaction: 65FA475AC6B006049190BF0B324A862C  
Result: passed  
Vendor ID: TeleSign  
Type: SMSAuth  
Performed: 25 January 2022 | 17:24  
Phone: +358 46 9206172

**Electronic Record and Signature Disclosure:**  
Not Offered via DocuSign

In Person Signer Events	Signature	Timestamp
<b>Editor Delivery Events</b>	<b>Status</b>	<b>Timestamp</b>
<b>Agent Delivery Events</b>	<b>Status</b>	<b>Timestamp</b>
<b>Intermediary Delivery Events</b>	<b>Status</b>	<b>Timestamp</b>
<b>Certified Delivery Events</b>	<b>Status</b>	<b>Timestamp</b>
<b>Carbon Copy Events</b>	<b>Status</b>	<b>Timestamp</b>
<b>Witness Events</b>	<b>Signature</b>	<b>Timestamp</b>
<b>Notary Events</b>	<b>Signature</b>	<b>Timestamp</b>
<b>Envelope Summary Events</b>	<b>Status</b>	<b>Timestamps</b>
Envelope Sent	Hashed/Encrypted	25 January 2022   14:52
Certified Delivered	Security Checked	25 January 2022   17:24
Signing Complete	Security Checked	25 January 2022   17:25
Completed	Security Checked	25 January 2022   17:25
<b>Payment Events</b>	<b>Status</b>	<b>Timestamps</b>